*Work supported in part by the U. S. Atomic Energy Commission.

†Work is based on a thesis submitted in partial fulfillment of the requirements for the degree of Doctor of Philosophy at the Carnegie Institute of Technology.

‡Present address: Plastics Department, E. I. du Pont de Nemours & Co., Parkersburg, W. Va. 26101.

[1]J. A. Rayne, Phys. Rev. 108, 22 (1957).
[2]J. A. Rayne, Phys. Rev. 110, 606 (1958).
[3]B. W. Veal and J. A. Rayne, Phys. Rev. 130, 2156 (1963).
[4]T. B. Massalski and L. L. Isaacs, Phys. Rev. 138, A139 (1965).
[5]M. A. Biondi and J. A. Rayne, Phys. Rev. 115, 1522 (1959).
[6]B. A. Green, Phys. Rev. 144, 528 (1966).
[7]L. C. Clune and B. A. Green, Phys. Rev. 144, 525 (1966).
[8]H. C. Yeh and L. V. Azaroff, J. Appl. Phys. 38, 4034 (1967).
[9]K. Fujiwara, O. Sueoka, and T. Imura, J. Phys. Soc. Japan 24, 467 (1968).
[10]P. E. King-Smith, Phil. Mag. 12, 1123 (1965).
[11]P. Soven, Phys. Rev. 151, 539 (1966).
[12]H. Amar, K. H. Johnson, and C. B. Sommers, Phys. Rev. 153, 655 (1967).
[13]M. L. Hammond, A. T. Davinroy, and M. I. Jacobson, Technical Report No. AFML-TR-65-223, 1965 (unpublished), p. 69.
[14]J. K. Lees and P. A. Flinn, J. Chem. Phys. 48, 882 (1968).
[15]S. L. Ruby, H. Montgomery, and C. W. Kimball, Phys. Rev. B 1, 2948 (1970).
[16]B. I. Verken, V. V. Chekin, and A. P. Vinnekov, Zh. Eksperim. i Teor. Fiz. 51, 25 (1966) [Soviet Phys. JETP 24, 16 (1967)].
[17]B. Window, J. Phys. C 2, 1 (1969).
[18]M. Cordey Hayes and I. R. Harris, Phys. Letters 24A, 80 (1967).

PHYSICAL REVIEW B VOLUME 3, NUMBER 3 1 FEBRUARY 1971

Three-Dimensional Scattering Analysis of Field Emission from a Tip. I. The Unperturbed Model*

Jay L. Politzer
Computation Center, The Pennsylvania State University, University Park, Pennsylvania 16802

and

T. E. Feuchtwang
Department of Physics, The Pennsylvania State University, University Park, Pennsylvania 16802

(Received 13 March 1970)

A formulation of field emission from a spherical tip is developed in terms of scattering theory. It is shown that in three dimensions the usual "transmission coefficient" is replaced by a differential scattering probability. The statistical average over the Fermi distribution is obtained without recourse to the usual kinetic arguments, which are shown to lack general validity. The zero-order problem is taken to be emission from a spherical well through a Coulomb barrier. This problem is solved exactly. The energy distribution of the field-emitted electrons is calculated for this model and found to be always larger than that calculated for the one-dimensional triangular barrier. In a second publication, more realistic models are analyzed in terms of a distorted-wave Born approximation which utilizes the solutions of the present problem.

I. INTRODUCTION

Recent work in field emission has stressed the observation and understanding of band-structure effects in the energy distributions of emitted electrons. This work is motivated by a desire to relate the observed distributions to the band structure of the emitting crystal. One impediment to an understanding of band-structure effects is that the only relevant experiment is field emission from fine needles or tips, while all of the theory has been developed for field emission from planar surfaces. Nevertheless, present indications from both theory and experiment are that band-structure effects do play a part in field emission, and that these effects are observable. Quantitative comparisons between theory and experiment are difficult to justify owing to the planar geometry used in the theory. In this paper, a three-dimensional theory of field emission is developed to account for more realistic emitter shapes. However, no attempt is made to account for the band structure of the emitter. We can assert, therefore, that differences between the present three-dimensional theory and experiment are probably due to band-structure effects alone, and are less likely to be attributable to the näive geometry of the theory. Conversely, it is not valid to assume that anomalies in field-emission data are due to band-struc-

ture effects unless all possible three-dimensional effects have been accounted for.

The most notable attempts to account for band structure in field emission were made by Itskovich[1-3] and Stratton.[4] Both of these authors consider field emission from a plane. Itskovich uses the actual Bloch functions inside the crystal, and the WKB transmission coefficient, to compute the emitted-energy distributions. He predicts angular variations of the energy distributions due to nonuniform emission from different portions of the constant-energy surfaces. Stratton uses the effective-mass approximation and the WKB transmission coefficient in his theory. His results depend upon cross sections of the constant-energy surfaces normal to the emission direction. This yields energy distributions which vary with the crystallographic orientation of the emitting surface. Swanson and Crouser[5-7] detected anomalies in the energy distributions of tungsten and molybdenum from particular crystal facets. They relate these anomalies to the topology of the constant-energy surfaces by means of Stratton's theory. Nagy and Cutler[8] show by calculation that Stratton's theory can qualitatively explain Swanson and Crouser's results. Because the anomalies do not appear on all crystal facets, it is unlikely that three-dimensional effects can account for them. This indicates that band-structure effects can indeed affect field emission. On the other hand, Whitcutt and Blott[9] measure large angular variations in the energy distributions of electrons field-emitted from copper deposited on tungsten. They maintain that these variations are consequences of the band structure of copper as shown by Itskovich's theory. This is unlikely because the implication of their paper is that the copper was deposited as a monolayer, and thin layers of a substance will probably not exhibit the band structure of the bulk.

In this paper, the emission tip is represented by a spherical well of constant potential in the region $r=0$ to $r=a$. A Coulomb barrier is assumed in the region $r=a$ to $r=\infty$. The Hamiltonian is then similar to that used in the study of α-particle decay, and is solved exactly without recourse to the WKB approximation. Field emission in this model is shown to be a scattering problem and is so treated. The invalidity of kinetic arguments in calculating incident particle flux for other than free particles in momentum eigenstates is demonstrated. The last point is of particular relevance in the three-dimensional treatment. The spherical geometry which is used precludes a convenient momentum-eigenstate representation, and the fluxes must be computed quantum mechanically. A consequence of the scattering formalism is that the familiar "transmission coefficient" is inadequate for the description of tunneling probabilities. It is superceded by the "differential scattering probability," the analog of the differential scattering cross section in ordinary scattering theory. The solutions to the above unperturbed Hamiltonian are used, in a second paper, as a basis for a perturbative treatment of more exact tunneling Hamiltonians.

II. ZERO-ORDER MODEL

We assume that the emission tip is a sphere. In the zero-order model, we consider tunneling in the one-electron potential

$$V=-W, \qquad r<a$$
$$=V_a(a/r-1), \quad R>r>a \ . \tag{2.1}$$

Here

$$V_a=V_0(1-a/R)^{-1}, \tag{2.2}$$

and V_0 is the potential applied between a spherical collector at $r=R\gg a$ and the surface of the tip at $r=a$. Since $R\gg a$, the potential about the tip is almost the same as for a collector at infinity. The field at the tip surface is

$$F_0=V_a/a \ . \tag{2.3}$$

The Schrödinger equation with the potential defined by Eq. (2.1) is separable in spherical coordinates, and the radial equation is[10]

$$Y_l''+\left(\alpha(E+W)-\frac{l(l+1)}{r^2}\right)Y_l=0, \qquad r<a \tag{2.4}$$
$$Y_l''+\left[\alpha\left(E+V_a-\frac{V_a a}{r}\right)-\frac{l(l+1)}{r^2}\right]Y_l=0, \qquad r>a.$$

Here $\alpha=0.26248$ for lengths in Å, energies in eV, fields in eV/Å, q in C, $\hbar$ in eV sec, and $\hbar/m$ in Å^2/sec. The Hamiltonian is virtually identical to that of an α particle tunneling out of a spherical nuclear well. The solutions of the angular equations are the spherical harmonics Y_l^m:

$$Y_l^m(\hat{r})=(-)^m\left[\frac{(2l+1)\,(l-m)!}{4\pi(l+m)!}\right]^{1/2}P_l^m(\cos\theta)e^{im\phi}, \tag{2.5}$$
$$0\le m\le l.$$

Here, P_l^m is the associated Legendre function, and $Y_l^{-|m|}$ is defined by

$$Y_l^{-|m|}(\hat{r})=(-1)^{|m|}\,Y_l^{|m|*}(\hat{r}). \tag{2.6}$$

The spherical harmonics form an orthonormal set on the unit sphere, i.e.,

$$\int Y_l^{m*}(\hat{r})Y_{l'}^{m'}(\hat{r})\,d\Omega=\delta_{mm'}\delta_{ll'}. \tag{2.7}$$

We may now solve Eq. (2.4) in the two regions $r<a$ and $r>a$.

(a) For $r<a$, possible solutions of the radial equation are[11]:

(i) spherical Bessel functions,

$$j_l(kr) = (\pi/2kr)^{1/2} J_{l+1/2}(kr) , \tag{2.8}$$

(ii) spherical Hankel functions of the first and second kind, [12]

$$h_l^{(+)}(kr) = (\pi/2kr)^{1/2} H^{(1)}_{l+1/2}(kr) \quad (= \text{outgoing wave}), \tag{2.9}$$

$$h_l^{(-)}(kr) = (\pi/2kr)^{1/2} H^{(2)}_{l+1/2}(kr) \quad (= \text{incoming wave}),$$

where

$$k^2 = \alpha(E+W).$$

The spherical Bessel functions do not carry any flux, and hence are not suitable for a barrier penetration problem. The spherical Hankel functions do represent outgoing and incoming waves, but these are singular at the origin. This singularity violates the condition of regularity at the origin which one normally imposes on solutions of the radial equation. Therefore, neither of the solutions (i) or (ii) appears to be a completely acceptable eigenfunction for the interior problem.

The resolution of this difficulty is not apparent in the case of α decay but may be achieved for field emission. In the statement of the present problem an essential element of the field electron microscope has been omitted from consideration – the wire connecting the tip through a potential source to the collector. That is, there is actually a source of, and sink for, electrons at the origin. Such singular sources and sinks may be handled by adding the physical stipulation that the flux of particles through a bounding surface about the singular source or sink remain finite in the limit as the bounding surface shrinks to zero. This is analogous to the manner in which point charges are handled in electrostatics.

In the following we make the physical assumption of such a δ-function source and sink at the origin. It is easy to verify that the total flux carried by $h_l^{(\pm)}$ waves through a bounding sphere is constant regardless of the sphere's radius, and that, therefore, the set $h_l^{(\pm)}$ is an acceptable solution to the interior radial equation.

(b) The solutions of Eq. (2.4) for $r>a$ are the Coulomb wave functions $G_l(\eta, Kr)$ and $F_l(\eta, Kr)$, where

$$K^2 = \alpha(E+V_a) \tag{2.10}$$

and

$$\eta = \alpha V_a a/2K. \tag{2.11}$$

These functions are discussed in Messiah. A suitable combination of the F_l and G_l which represents an asymptotically outgoing (+), or incoming (–), wave is

$$C_l^{(\pm)} = (G_l \pm iF_l)/Kr. \tag{2.12}$$

Thus

$$\psi = Y_l^m[\, I_l h_l^{(+)}(kr) + R_l h_l^{(-)}(kr)], \quad r<a \tag{2.13}$$

$$\psi = Y_l^m T_l C_l^{(+)}(Kr), \quad r>a \tag{2.14}$$

where I_l, R_l, and T_l are the incident, reflected, and transmitted wave amplitudes.

III. MATCHING CONDITIONS

T_l and R_l in Eqs. (2.13) and (2.14) are determined by demanding that ψ and $\vec{\nabla}\psi$ be continuous at the boundary $r=a$. Since the angular solutions are the same inside and outside the sphere, the matching conditions become

$$\frac{I_l}{T_l} h_l^{(+)} + \frac{R_l}{T_l} h_l^{(-)} = C_l^{(+)}, \tag{3.1}$$

$$\frac{I_l}{T_l} h_l^{(+)\prime} + \frac{R_l}{T_l} h_l^{(-)\prime} = \frac{K}{k} C_l^{(+)\prime}, \tag{3.1$'$}$$

where all functions are evaluated at $r=a$, and the prime denotes differentiation with respect to the argument, i.e.,

$$' = \frac{\partial}{\partial kr} \quad \text{for } h_l^{(\pm)}$$

$$= \frac{\partial}{\partial Kr} \quad \text{for } C_l^{(\pm)} .$$

In the energy range of interest, the NBS asymptotic forms for $h_l^{(-)}$ and $C_l^{(+)}$ may be used to solve Eqs. (3.1). These asymptotic forms are valid when

$$1/ka \ll 1 \quad \text{for } h_l^{(-)}$$

and

$$\left| \frac{Ka - 2\eta}{2\eta} \right| \ll 1 \quad \text{for } C_l^{(+)} .$$

In our case,

$$1/ka \approx 2a^{-1}(E+W)^{-1/2}$$

and

$$\left| \frac{Ka - 2\eta}{2\eta} \right| = \frac{-E}{V_a} \approx 10^{-2}\text{–}10^{-3} ,$$

where a was taken to be 500 Å, $E \sim \frac{1}{2} W \sim 5$ eV. Thus the use of the asymptotic forms is justified. After considerable algebraic work, we obtain

$$\frac{T_l}{I_l} \approx 2\left[\frac{-E}{E+W}\right]^{1/2} \frac{[-E/(E+W)]^{1/2} - i}{1 - E/(E+W)} \left(\frac{V_a}{-E}\right)^{1/4} \times e^{ika} \exp\left(-\frac{2}{3}\frac{\alpha^{1/2}}{F_0}(-E)^{3/2}\right) (-i)^l \tag{3.2}$$

and

$$\frac{R_l}{I_l} \approx \frac{-\{1+i[-E/(E+W)]^{1/2}\}^2}{1-E/(E+W)} e^{2ika}(-)^l. \quad (3.3)$$

For later use we set $I_l = 1$ and define the l-independent quantities T and R:

$$T = T_l(i)^l, \quad (3.4)$$

$$R = R_l(-)^l. \quad (3.5)$$

IV. FIELD EMISSION AS A SCATTERING PROBLEM: "DIFFERENTIAL SCATTERING PROBABILITY"

In one-dimensional problems the transmission coefficient is the ratio of the transmitted flux to the incident flux. For one-dimensional problems the "transmission coefficient" is well defined because the transmitted current is uniform over any plane parallel to the emission plane, and conservation of current implies that the current is position independent in the outside region. For the wave functions in Sec. II, however, the current is a function of both angle and radius. Further, the quantity of interest is the "differential scattering probability," i.e., the probability that a given incident particle will be detected at position $\vec{r}$. This is more detailed information than the mere knowledge of the probability that the particle will penetrate the barrier. This point is clarified by comparing our problem to a scattering experiment involving a planar beam of particles incident on a target. The transmission coefficient is analogous to the total cross section, that is, the probability that particles in the incident beam get scattered at all. On the other hand, the differential scattering probability is analogous to the differential scattering cross section, which is a measure of the probability that particles are scattered into a particular differential solid angle. In our problem, the electrons incident on the barrier from the inside are represented by spherical waves which carry both radial and angular momenta. The transmitted electrons are distributed nonuniformly throughout the space external to the sphere. In order to characterize these electrons we require the analog of the differential scattering cross section of ordinary scattering theory.

Consider a solid angle Ω intercepting an area S' on the tip and an area S on a sphere of radius r. Here S is to represent the aperture of a detector which registers all particles striking it. Not all particles that are incident at S' will reach S because the barrier may scatter some of these particles out of Ω. Conversely, particles striking the barrier at some area other than S' may subsequently get scattered by the barrier into Ω, and these may reach S. In fact, only those particles which maintain zero angular momentum will pass through both S and S'. In order to account for all of the above possibilities we introduce the scattering probability $\sigma(k, l, m)$ that a particle with quantum numbers (k, l, m) is detected at S. This probability is the ratio of the current of such particles crossing S to the current of such particles incident on the entire barrier.

With $\vec{J}_T$ the expectation value of the current operator for the transmitted wave, and $\vec{J}_I$ the same quantity for the incident wave, the current of particles crossing S is

$$r^2 \int_S \vec{J}_T \cdot \hat{r}\, d\Omega, \quad (4.1)$$

while the incident current at the barrier is

$$\int \vec{J}_I \cdot d\vec{A}. \quad (4.2)$$

The integral in Eq. (4.2) is over the surface of the entire tip. We now define

$$\sigma = r^2 \int_S \vec{J}_T \cdot \hat{r}\, d\Omega / \int \vec{J}_I \cdot d\vec{A} \quad (4.3)$$

and differentiating the right-hand side with respect to Ω, we obtain the differential scattering probability

$$\frac{d\sigma}{d\Omega} = \frac{r^2 \vec{J}_T \cdot \hat{r}}{\int \vec{J}_I \cdot d\vec{A}}. \quad (4.4)$$

Using Eqs. (2.13) and (2.14) the differential scattering probability reduces to

$$\frac{d\sigma}{d\Omega} = \left|\frac{T_l}{I_l}\right|^2 \frac{k}{K} Y_l^{m*} Y_l^m. \quad (4.5)$$

We now define the total transmission probability $\sigma_T(k, l, m)$ to be the probability that the (k, l, m) particle will be detected any place at all outside of the tip, i.e.,

$$\sigma_T(k, l, m) = \int \frac{d\sigma}{d\Omega}\, d\Omega, \quad (4.6)$$

where the integral is over a sphere of radius $r > a$. Using Eq. (2.7),

$$\sigma_T(k, l, m) = \left|\frac{T_l}{I_l}\right|^2 \frac{k}{K}. \quad (4.7)$$

Therefore we can rewrite Eq. (4.5) as

$$\frac{d\sigma}{d\Omega} = \sigma_T Y_l^{m*}(\hat{r}) Y_l^m(\hat{r}). \quad (4.8)$$

Finally, substituting Eqs. (3.2) and (4.7) into Eq. (4.8) we obtain

$$\frac{d\sigma}{d\Omega} \approx \frac{4[-E(E+W)]^{1/2}}{W} \exp\left(-\frac{4}{3}\frac{\alpha^{1/2}}{F_0}(-E)^{3/2}\right) Y_l^{m*} Y_l^m. \quad (4.9)$$

This shows that $\sigma_T(k, l, m)$ is only a function of the energy, i.e., of k. Thus σ_T appears to be equivalent to the transmission coefficient of one-dimensional problems.

It must be pointed out that in general $\sigma_T(k, l, m)$, the probability that the particle may be found anywhere at all outside, is not completely equivalent to the ordinary one-dimensional transmission co-

efficient. The reason for this is that σ_T could in principle exhibit a dependence on the quantum numbers (l, m). It is accidental that in our example this dependence drops out. The one-dimensional transmission coefficient therefore may not be compared directly with σ_T but only to its average over the quantum numbers (l, m). In the following, comparisons are made between the three-dimensional and one-dimensional energy distributions rather than between σ_T and the one-dimensional transmission coefficient. This is done because the energy distribution is a physical observable, while σ_T or the one-dimensional transmission coefficient must be inferred from the experimental data.

V. STATISTICS AND MONOCHROMATIC SUPPLY FUNCTION

We must now relate the differential scattering probability to experimentally observable detector currents. This requires an enumeration of the internal states of the spherical tip and a definition of the averaging procedure over these states. The states that were chosen to compute the differential scattering probability represent traveling waves and are not localized in the tip. This makes them awkward to use in a discussion of the statistics. We will therefore compute the detected current in a manner similar to that used in one-dimensional problems. For the moment we assume the existence of a detector capable of discriminating the partial monochromatic current of particles all having the same quantum numbers (k, l, m).

From Eq. (4.4), the detected radial component of the electric current density $J(k, l, m, \vec{r})$ of particles with quantum numbers (k, l, m) at the position $\vec{r}$ is

$$J(k, l, m, \vec{r}) = \frac{qI(k, l, m)}{r^2} \frac{d\sigma}{d\Omega}(k, l, m, \hat{r}), \tag{5.1}$$

where q is the electron charge and $I(k, l, m)$ is the radial component of the total particle current of (k, l, m) particles incident at the barrier. Possible deviations of the electronic distribution in the tip due to transport effects will be neglected and $I(k, l, m)$ will be computed for the thermal equilibrium distribution in the tip.

In one-dimensional problems it has been the practice[13,14] to compute incident fluxes on the basis of "kinetic arguments." In effect, these arguments use the classical expression

$$\vec{J} = \rho \vec{v}, \tag{5.2}$$

instead of the quantum-mechanical current density. (Here $\vec{J}$ is the current density, ρ is the density of particles, and $\vec{v}$ is their velocity.) In plane-wave states it is clear that

$$\rho = \psi\psi^* = \text{const}. \tag{5.3}$$

Because the plane waves are momentum eigenstates, the quantum-mechanical flux is then the same as that given by Eq. (5.2) with suitable normalization. When $\psi\psi^*$ is not constant and we do not have momentum eigenstates, the classical expression fails to represent the quantum-mechanical expression for the flux and is therefore incorrect. In light of this, the kinetic argument must be abandoned in favor of a purely quantum-mechanical expression for the flux.

To proceed with the calculation of $I(k, l, m)$, the internal states of the tip in the absence of an emitted current must be investigated. In contrast with the development in Sec. II, now there are no electron sources or sinks, and the spherical Hankel functions are no longer acceptable eigenstates. The free-particle eigenstates can only be

$$\psi = Y_l^m j_l(kr). \tag{5.4}$$

Further, k must be quantized by applying appropriate boundary conditions on the solutions given by Eq. (5.4). We assert that at $r = a$

$$\psi(a) = 0, \tag{5.5}$$

which corresponds to putting an impenetrable wall at the tip boundary. The quantization condition for k is therefore

$$k = j_{l+1/2,n}/a, \quad n = 1, 2, \ldots \tag{5.6}$$

where $j_{l+1/2,n}$ is the nth root of the lth Bessel function. Thus, the wave functions, which are orthonormalized in the volume of the tip, become

$$\psi_{nlm} = \left(\frac{4 j_{l+1/2,n}}{\pi a^3 J'^2_{l+1/2}(j)_{l+1/2,n}}\right)^{1/2} \times \{Y_l^m(\hat{r}) j_l[j_{l+1/2,n}\, r/a]\}. \tag{5.7}$$

As was previously noted, the states ψ_{nlm} represent standing waves and carry no current. Alternatively, these states may be viewed as transporting equal and opposite fluxes in the directions $+\hat{r}$ and $-\hat{r}$, the net flux being zero. We adopt the latter viewpoint to calculate the flux incident on the barrier in the $+\hat{r}$ direction. Using the decomposition

$$j_l \equiv \tfrac{1}{2}(h_l^{(+)} + h_l^{(-)}), \tag{5.8}$$

the incident flux at position $\hat{a}$ on the tip is

$$\frac{\hbar\, Y_l^{m*}(\hat{a}) Y_l^m(\hat{a})}{m_e \pi a^4 J'^2_{l+1/2}(j_{l+1/2,n})}. \tag{5.9}$$

The incident current is then the integral of Eq. (5.9) over the surface of the tip. Using Eq. (2.7), the incident current per particle is

$$\frac{\hbar}{m_e \pi a^2 J'^2_{l+1/2}(j_{l+1/2,n})}. \tag{5.10}$$

The total incident particle current $I(n, l, m)$ is the incident current per particle, Eq. (5.10), times

the number of (n,l,m) particles in the volume of the tip. The latter quantity is the number of (n, l, m) states in the volume (two for particles of spin one-half) times the probability of occupancy of the state [the Fermi-Dirac distribution $f(E_{n,l})$]. Thus,

$$I(n, l, m) = \frac{2\hbar f(E_{n,l})}{m_e \pi a^2 J'^2_{l+1/2}(j_{l+1/2,n})} . \tag{5.11}$$

Finally, substituting Eq. (5.11) and Eq. (4.8) into Eq. (5.1), the detected electric current density of (n, l, m) particles is

$$J(n, l, m) = \frac{2\hbar q f(E_{n,l}) \sigma_T(E_{n,l}) Y_l^{m*}(\hat{r}) Y_l^m(\hat{r})}{m_e \pi r^2 a^2 J'^2_{l+1/2}(j_{l+1/2,n})} . \tag{5.12}$$

VI. ENERGY DISTRIBUTION

Equation (5.12) is unsatisfactory from an experimental viewpoint because there is no detector capable of discriminating particles with different quantum numbers (n, l, m). An expression for the current due to all electrons with energies between E and $E + \Delta E$ is required. Because of the axial symmetry of the problem, the energy is not a function of the quantum number m. The current density of all (n, l) particles may therefore be obtained by summing Eq. (5.12) over all $-l \le m \le l$. From the identity

$$\sum_{m=-1}^{m=1} Y_l^{m*}(\hat{r}) Y_l^m(\hat{r}) = \frac{2l+1}{4\pi} , \tag{6.1}$$

we obtain

$$J(n, l) = \frac{\hbar q f(E_{n,l}) \sigma_T(E_{n,l})(2l+1)}{2 m_e \pi^2 r^2 a^2 J'^2_{l+1/2}(j_{l+1/2,n})} . \tag{6.2}$$

In principle, the current due to all electrons with energies between E and $E + \Delta E$ may be obtained by performing the sum

$$\Delta J(E) = \sum_{n,l} J(n, l), \tag{6.3}$$

where n and l range over the region of n-l space between the curves $E = \text{const}$ and $E + \Delta E = \text{const}$. If $\Delta E \ll 1$, this may be written

$$P_3^0(E)\Delta E = \sum_{n,l} J(n, l) , \tag{6.4}$$

where $P_3^0 = \Delta J / \Delta E$ is the energy distribution for the zero-order three-dimensional Hamiltonian. Using NBS (9.2.1) and (9.2.11), and Eq. (5.6), we obtain

$$J'^2_{l+1/2}(j_{l+1/2,n}) \approx 2/\pi k a, \tag{6.5}$$

which is valid for

$$\lim_{l=\text{const},\, n\to\infty} j_{l+1/2,n} .$$

In practice Eq. (6.5) is satisfied for all but the first few zeros of $J_{l+1/2}$. Therefore,

$$P_3^0(E) = \frac{\hbar q f(E) \sigma_T(E) k}{4 m \pi r^2 a \Delta E} \sum_{n,l} (2l+1). \tag{6.6}$$

We now observe that the number of electrons per unit volume in the sphere with energies between E and $E + \Delta E$ is

$$\rho_s(E)\Delta E = \frac{3 f(E)}{2\pi a^3} \sum_{n,l} (2l+1) . \tag{6.7}$$

The analogous quantity for a cube is

$$\rho_c(E)\Delta E = \alpha f(E) k \Delta E / 2\pi^2. \tag{6.8}$$

For a free-electron gas, in a macroscopic volume, the Fermi energy is only a function of the total electron density. For a cube and a sphere of the same material at 0 °K, this density is

$$\int_{-\infty}^{-E_F} \rho_c(E)\, dE = \int_{-\infty}^{-E_F} \rho_s(E)\, dE . \tag{6.9}$$

Since E_F is arbitrary, we conclude that

$$\rho_c(E) = \rho_s(E) . \tag{6.10}$$

Finally, using Eqs. (6.10), (6.6)–(6.8), and substituting for σ_T the right side of Eq. (4.7), we obtain

$$P_3^0(E) = \frac{\hbar q \alpha^2 (a/r)^2 f(E)[-E(E+W)^3]^{1/2}}{3 m_e \pi^2 W} \times \exp\left(\frac{-4\alpha^{1/2}(-E)^{3/2}}{3F_0}\right). \tag{6.11}$$

Numerically,

$$P_3^0(E)\frac{A}{\text{Å}^2 - \text{eV}} = 4.32\times 10^{-6}\left(\frac{a}{r}\right)^2 f(E)\frac{-E(E+W)^3}{W} \times \exp\left(\frac{-0.6831(-E)^{3/2}}{F_0}\right) . \tag{6.12}$$

VII. COMPARISON OF ZERO-ORDER THREE-DIMENSIONAL AND ONE-DIMENSIONAL ENERGY DISTRIBUTIONS

The simple triangular barrier is chosen for comparison with the spherical Coulomb barrier. The transmission coefficient for the triangular barrier is[15]

$$D = \frac{4}{W}[-\epsilon(\epsilon+W)]^{\frac{1}{2}} \exp\left(-\frac{4}{3}\frac{\alpha^{1/2}(-\epsilon)^{3/2}}{F_0}\right) , \tag{7.1}$$

where

$$\epsilon = E - (\hbar k_\perp)^2/2m_e , \tag{7.2}$$

and $k_\perp$ is the transverse k vector. Using Young's analysis[16] and Eq. (7.1), the energy distribution for the triangular barrier is

$$P_1^0 = \frac{16\pi m_e q}{W h^3} f(E) \int_{-W}^{E} [-\epsilon(\epsilon+W)] \times \tfrac{1}{2} \exp\left(-\frac{4}{3}\frac{\alpha^{1/2} W^{3/2}(-\epsilon/W)^{3/2}}{F_0}\right) d\epsilon . \tag{7.3}$$

Since the quantity

$$\gamma=\frac{4}{3}\frac{\alpha^{1/2}W^{3/2}}{F_0}\gg 1\ ,$$

the integral in Eq. (7.2) may be approximately evaluated, and we obtain

$$P_1^0\approx\frac{m_e q}{\pi^2\hbar^3\alpha^{1/2}}\frac{F_0}{W}(E+W)^{1/2}f(E)$$
$$\times\exp\left(-\frac{4}{3}\frac{\alpha^{1/2}}{F_0}(-E)^{3/2}\right)\ . \qquad (7.4)$$

Evaluating all numerical constants we have

$$\frac{P_1^0}{\frac{A}{\text{Å}^2-\text{eV}}}\approx 6.32\times10^{-6}\frac{F_0}{W}(E+W)^{1/2}f_{(E)}$$
$$\times\exp\left(\frac{-0.6831(-E)^{3/2}}{F_0}\right)\cdot \qquad (7.5)$$

For the energy ranges accessible to experiment, the pre-exponential factors in P_3^0 and P_1^0 are nearly constant and the energy dependence of both distributions is essentially exponential. Indeed, the WKB approximation gives the same exponential energy dependence without the prefactors. Because of the limited range of variability of the prefactors, and the dominance of the exponential, we cannot expect to discriminate between the distributions P_3^0 and P_1^0 on the basis of a simple experiment. P_3^0 is compared with P_1^0 in Fig. 1, at $r=a$ and at 0 °K. It is seen that P_3^0 is always greater than P_1^0 in the energy range of interest. Furthermore,

$$\frac{P_3^0}{P_1^0}=\frac{0.68(E+W)\sqrt{-E}}{F_0}\ , \qquad (7.6)$$

which peaks at $E=-\frac{1}{3}W$. Therefore,

$$P_3^0\leqq 1.36(\tfrac{1}{3}W)^{3/2}P_1^0/F_0\ . \qquad (7.7)$$

P_3^0 and P_1^0 represent the two extreme geometrical limits for the field emission problem. The displacements between these distributions and their different preexponential energy dependences are direct consequences of three-dimensional effects. P_3^0 is the energy distribution for a finite sphere of radius a with a spherical collector of radius R. P_1^0 is the energy distribution for an infinite plane with a planar collector at a distance d from it. In principle, P_1^0 may be obtained from P_3^0 in the limit $a\to\infty$, $R\to\infty$, while $R-a=d$, and $F_0=$ const. However, implicit in the present calculation for P_3^0 is the limit $R\to\infty$ while a is bounded. Therefore, P_1^0 may not be obtained from P_3^0, as given by Eq. (6.12), by letting a tend to infinity subject to the above constraints. On the basis of the foregoing, it is expected that calculation of P_3^0 in the intermediate range $a\approx R\to\infty$ would yield energy distributions intermediate between P_1^0 and P_3^0 in Eq. (6.12).

VIII. CONCLUSIONS

In this paper a completely three-dimensional analysis of field emission has been achieved for the first time. The Coulomb barrier was used for an unperturbed model Hamiltonian. It was shown that quantum-mechanical δ-function particle sources and sinks could be accommodated within the mathematics, and the α-particle Hamiltonian was solved exactly. The concept of the "differential scattering probability" was introduced within the context of scattering theory. The relationship of this notion to the one-dimensional transmission coefficient was discussed. It was demonstrated that the quantum-mechanical expression for the flux must be used in developing the statistical averaging, and that the usual kinetic arguments have no general validity. Finally, the energy distribution for the Coulomb barrier was derived and compared with the distribution predicted for a one-dimensional triangular barrier. The comparison revealed that both energy distributions contain the same exponential energy dependence, with different preexponential factors. It was therefore concluded that the apparent success of one-dimensional treatments is due to the fact that most experiments are insensitive to the preexponential factors.

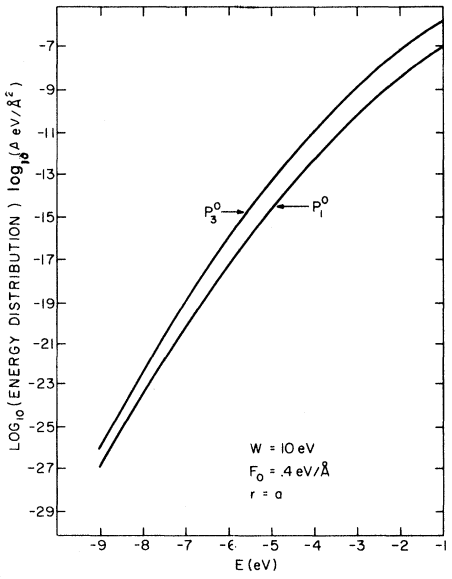

FIG. 1. Comparison of the one- and three-dimensional energy distributions at the emitting surface for a typical value of the electric field. The cutoff at the Fermi energy is not shown.

In a following publication, a perturbation theoretic viewpoint is adopted to determine the effect of image forces, patch fields, etc., on the energy distribution. Specifically, the eigenfunctions of the unperturbed Hamiltonian are used to construct a Green's function. This in turn is approximated and used to solve the perturbed Hamiltonian. This new method of treating tunneling problems leads to the "integral equation for tunneling," in analogy to the parallel development in scattering theory,

which leads to the "integral equation for scattering." Using this formalism it is shown that the resultant energy distribution differs from that of the one-dimensional treatment because of the appearance of additional energy- and angle-dependent pre-exponential factors.

---

*Research sponsored by the Air Force Office of Scientific Research, Office of Aerospace Research, U.S. Air Force, under AFOSR Contract/Grant No. AFOSR-69-1727.

[1]F. I. Itskovich, Zh. Eksperim. i Teor. Fiz. 50, 1425 (1966) [Soviet Phys. JETP 23, 945 (1966)].

[2]F. I. Itskovich, Zh. Eksperim. i Teor. Fiz. 51, 301 (1966) [Soviet Phys. JETP 24, 202 (1967)].

[3]F. I. Itskovich, Zh. Eksperim. i Teor. Fiz. 52, 1720 (1967) [Soviet Phys. JETP 25, 1143 (1967)].

[4]R. Stratton, Phys. Rev. 135, A794 (1964).

[5]L. W. Swanson and L. C. Crouser, Phys. Rev. Letters 16, 389 (1966).

[6]L. W. Swanson and L. C. Crouser, Phys. Rev. Letters 19, 1179 (1967).

[7]L. W. Swanson and L. C. Crouser, Phys. Rev. Letters 163, 622 (1967).

[8]D. Nagy and P. Cutler, Phys. Rev. 185, (1969).

[9]R. D. B. Whitcutt and B. H. Blott, Phys. Rev. Letters 23, 639 (1969).

[10]A. Messiah, *Quantum Mechanics* (North-Holland, Amsterdam, 1962), Vol. I, Chap. IX, and Appendixes. (We will refer to Chapters IX, XI, XIX, and the Appendixes in Vols. I and II of this book as Messiah.)

[11]*Handbook of Mathematical Functions*, edited by M. Abramowitz and I. Stegun, Nat. Bur. Std. Applied Math Series No. 55 (U.S. GPO, Washington, D. C., 1964), Chap. 10. [We will refer to Chaps. 8–11 and 14 of this book as NBS and refer to some NBS equations by their equation numbers, e.g., NBS (10.3) is NBS equation number (10.3).]

[12]The functions defined here as $h_l^{(\pm)}$ differ by a phase factor from those defined by Messiah and correspond to the NBS $h_l(\frac{1}{2})$.

[13]R. H. Good and E. W. Mueller, in *Handbuch der Physik*, edited by S. Flügge (Springer, Berlin, 1956), Vol. 21, p. 181.

[14]R. Young, Phys. Rev. 113, 110 (1959).

[15]L. Nordheim, Proc. Roy. Soc. (London) 121, 638 (1928).

[16]See Ref. 14.

PHYSICAL REVIEW B VOLUME 3, NUMBER 3 1 FEBRUARY 1971

Numerical Solution of the Equation Governing Nuclear Magnetic Spin-Lattice Relaxation in a Paramagnetic-Spin-Doped Insulator*

J. I. Kaplan

Columbus Laboratories, Battelle Memorial Institute, 505 *King Avenue, Columbus, Ohio* 43201

(Received 16 June 1970)

A numerical solution of the equation

$$\frac{\partial M^z}{\partial t} = D\left(\frac{1}{r}\frac{\partial^2}{\partial r^2}(rM^z)\right) - \frac{(M^z - M_0^z)\bar{C}}{r^6}$$

governing nuclear relaxation in a paramagnetic-spin-doped insulator has been obtained. The results are expressed in terms of

$$\bar{m}(t) = \int_b^R [M_0^z - M^z(t)]\, r^2\, dr \Big/ \int_b^R M_0^z r^2\, dr \quad ,$$

where $M^z(0) = 0$, b is the so-called "diffusion barrier" and $(4\pi R^3/3)^{-1}$ equals the paramagnetic-spin concentration. Simple analytic forms for the long-time exponential decay of $\bar{m}(t)$ are obtained for either D or $\bar{C}$ dominating the relaxation process. Graphical solutions for the intermediate regions are also obtained. The short-time nonexponential solution of $\bar{m}(t)$ is discussed.

INTRODUCTION

Bloembergen[1] and others[2] have argued that the differential equation governing nuclear spin-lattice relaxation in an insulator with a low concentration of paramagnetic spins is

$$\frac{\partial M^z}{\partial t} = D\left(\frac{1}{r}\frac{\partial^2}{\partial r^2}(rM^z)\right) - \frac{M^z - M_0^z}{T_1(r)} \quad , \tag{1}$$

where M_0^z is the equilibrium nuclear magnetization and

$$T_1(r)^{-1} = \langle 3(\gamma_e\gamma_n\hbar)^2 S(S+1) r^{-6} \sin^2\theta \cos^2\theta [\tau(1+\omega_0^2\tau^2)^{-1}] \rangle$$
$$= \bar{C}\tau(1+\omega_0^2\tau^2)^{-1} \quad , \tag{2}$$

where $\langle\,\rangle$ means angular average, D is the spin-diffusion constant, ω_0 is the nuclear Larmor frequency, and $\vec{r} = 0$ defines the location of a paramagnetic impurity. The boundary conditions defining the solution of Eq. (1) are

$$M^z(r, o) = 0, \tag{3}$$

which indicates saturation of the nuclear spin